

Numerical Analysis of a Nonlinear Vibrating Two-Degrees-of-Freedom System with Various Friction Models

¹Kanita Lemes, ²Dzanko Hajradinovic, ³Marin Petrovic

¹MSc Student, Mechanical Engineering Faculty, University of Sarajevo, Bosnia and Herzegovina

²Senior research assistant, Mechanical Engineering Faculty, University of Sarajevo, Bosnia and Herzegovina

³Associate professor, Mechanical Engineering Faculty, University of Sarajevo, Bosnia and Herzegovina

Abstract - The dynamics of the two-degrees-of-freedom system, constituted of two bodies interacting with the weightless plate having harmonic displacement in different environments, is analyzed in this paper. Resistance of the environment is described by four different friction models: Coulomb friction model, Coulomb viscous model, Coulomb-Stribeck model and the LuGre friction model. The paper is mainly focused on changes in vibration of masses depending on the friction model. The analysis is conducted by monitoring displacements of the masses and phase-space diagrams.

Keywords: Vibration, friction, Coulomb friction, Stribeck effect, LuGre model.

I. INTRODUCTION

This paper studies a vibration of a system constituted of two bodies interacting with a harmonically driven weightless plate in various environments described by four friction models. They are Coulomb friction model, Coulomb viscous model, Coulomb-Stribeck model and LuGre friction model. Not much work on this topic has been performed so far and the literature related to such kind of analyses is relatively scarce. It is well known that a friction between solid bodies is an extremely complicated physical phenomenon. It encompasses elastic and plastic deformations of surface layers of contacting bodies, interactions with wear particles, micro-fractures and a restoration of a continuity of materials, chemical reactions, and the transfer of particles from one body to another [1].

The Coulomb friction model is a simple model of dry friction and, according to this model, the friction force is proportional to the normal force and it is independent of the contact area. The Coulomb viscous model is employed in the presence of lubricants. The lubricants provide a fluid barrier between rubbing metal parts which replace dry friction with viscous friction and may vastly reduce wear [2]. The friction

force, according to this model, is proportional to the relative velocity between the bodies in contact.

The friction force may vary at low values of the relative velocity when the thickness of the lubricant is large enough to completely separate the contacting bodies and hydrodynamic effects become significant. This effect is recognized as the Stribeck effect [3]. The Coulomb-Stribeck model, representing combination of the Coulomb friction and the Stribeck effect, provides appropriate presentation of the friction at low velocity. However, in the vicinity of zero relative velocity, it lacks a physical representation of the friction. The representation of the friction, according to the LuGre model, is based on the interaction between contacting surfaces on the microscopic level. The nature of friction depends on the relationship between asperities and it is modeled by means of their elastic deformations.

Important characteristic of vibrating system is the time period to reach the steady state motion. This time period depends on the dissipation of energy from the system. The mechanical system has two energy dissipaters in form of a viscous damper and different frictions. This paper shows how fast the system transits to the steady state motion for different friction models and an amplitude of oscillations. Similar physical system was analyzed in [4-7] where the excitation is caused by vibro-impact motion.

Their goal was to show the way the vibro-impact system is used to govern certain system, as well as influence of different friction models on analyzed vibro-impact system. In this paper the excitation source is a harmonic displacement function which may be produced by an electromotor through a simple operating mechanism. The aim is to explain an influence of different friction models on vibrating motion caused, simulating different environments in which the vibrating system may operate.

II. MATHEMATICAL AND PHYSICAL MODELLING

In this work, two degrees-of-freedom system is considered, shown in Fig. 1, where weightless plate has a harmonic displacement with amplitude u_o and frequency Ω_p .

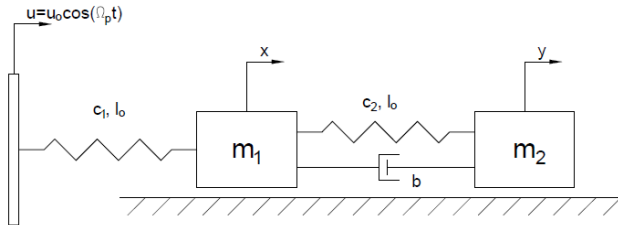


Figure 1: Physical model of two-degrees-of-freedom system

The weightless plate interacts with a mass 1 via linear spring with stiffness c_1 . Mass 1 is connected to the mass 2 by a linear spring with stiffness c_2 and a viscous damper with damping coefficient b . The motion of the system is completely described by coordinates $x(t)$ and $y(t)$, defining the positions of the masses m_1 and m_2 at any time t from the respective equilibrium positions. Bidirectional motion of the mass 1 and mass 2 will occur when the forces acting on the bodies exceed the threshold of the friction forces between bodies and the supporting environmental surface.

Equations of motion of the system are given by the Lagrange equation:

$$\frac{d}{dt} \left(\frac{\partial E_k}{\partial \dot{q}_i} \right) - \frac{\partial E_k}{\partial q_i} + \frac{\partial E_p}{\partial q_i} = Q_i, i = 1, 2, \dots, s,$$

where E_k is kinetic energy of the system, E_p is potential energy of the system, q_i is generalized coordinate, \dot{q}_i is generalized velocity, t is time, Q_i is generalized force and s is number of degrees of freedom of the system.

Kinetic energy of the system is:

$$E_k = \frac{1}{2} m_1 \dot{x}^2 + \frac{1}{2} m_2 \dot{y}^2$$

Potential energy of the system is:

$$E_p = \frac{1}{2} c_1 (x - u)^2 + \frac{1}{2} c_2 (y - x)^2$$

$$E_p = \frac{1}{2} c_1 (x - u_o \cos(\Omega_p t))^2 + \frac{1}{2} c_2 (y - x)^2$$

Where μ is friction coefficient, m_1 and m_2 are masses of the body 1 and body 2, respectively, g is gravitational acceleration and c_1 and c_2 are stiffness of the spring 1 and spring 2, respectively.

A) Coulomb model

According to Coulomb model, when the contact surface between two solids is dry, friction force has a constant value and it is acting in the direction opposite to the relative velocity [8]. Friction force F_μ is proportional to the normal contact force N [9].

Differential equations of motion are given by:

$$m_1 \ddot{x} + b \dot{x} - b \dot{y} + (c_1 + c_2)x - c_2 y + \mu m_1 g \text{sign}(\dot{x}) = c_1 u_o \cos(\Omega_p t)$$

$$m_2 \ddot{y} + b \dot{y} - b \dot{x} + c_2 y - c_2 x + \mu m_2 g \text{sign}(\dot{y}) = 0$$

B) Coulomb viscous model

When the contact surface between two solids is covered with a thin liquid film so that the two surfaces do not touch, it is usual to assume that the friction force is proportional to the relative velocity of two bodies. It is often combined with Coulomb friction [10].

Differential equations of motion are given by:

$$m_1 \ddot{x} + (b + K \text{sign}(\dot{x})) \dot{x} - b \dot{y} + (c_1 + c_2)x - c_2 y + \mu m_1 g \text{sign}(\dot{x}) = c_1 u_o \cos(\Omega_p t)$$

$$m_2 \ddot{y} + (b + K \text{sign}(\dot{y})) \dot{y} - b \dot{x} + c_2 y - c_2 x + \mu m_2 g \text{sign}(\dot{y}) = 0$$

C) Coulomb-Stribeck model

The Stribeck effect represents decreasing friction with increasing velocity at low velocity during transition from static to kinetic friction. A combination of static friction, Coulomb and viscous friction model is been referred to as Stribeck friction [11]. Differential equations of motion are:

$$m_1 \ddot{x} + b \dot{x} - b \dot{y} + (c_1 + c_2)x - c_2 y + (\mu m_1 g + (\mu_s - \mu) m_1 g e^{-|\dot{x}|^{1/\delta}}) \text{sign}(\dot{x}) = c_1 u_o \cos(\Omega_p t)$$

$$m_2 \ddot{y} + b \dot{y} - b \dot{x} + c_2 y - c_2 x + (\mu m_2 g + (\mu_s - \mu) m_2 g e^{-|\dot{y}|^{1/\delta}}) \text{sign}(\dot{y}) = 0$$

D) LuGre model

The LuGre friction model is the dynamic friction model. Friction is modeled as the average deflection force of elastic springs. This models the phenomenon that the surfaces are pushed apart by the lubricant and model the Stribeck effect [12]. Differential equations of motion are now:

$$m_1 \ddot{x} + (b + \sigma_2) \dot{x} - b \dot{y} + (c_1 + c_2)x - c_2 y + \sigma_o z_1 + \sigma_1 \frac{dz_1}{dt} = c_1 u_o \cos(\Omega_p t)$$

$$m_2 \ddot{y} + (b + \sigma_2) \dot{y} - b \dot{x} + c_2 y - c_2 x + f m_2 g \text{sign}(\dot{y}) + \sigma_o z_2 + \sigma_1 \frac{dz_2}{dt} = 0$$

III. DYNAMIC ANALYSIS AND DISCUSSION

In order to understand the system dynamics in different friction environments, this section shows various responses of the system with four different frictions. The results are presented on two different diagrams for each body: 1) where the displacement is plotted on the y-axis as a function of time and 2) space-phase diagram, where velocity is plotted on the y-axis as a function of displacement. The calculations were run for 15 seconds of motion of the system.

A) Coulomb model

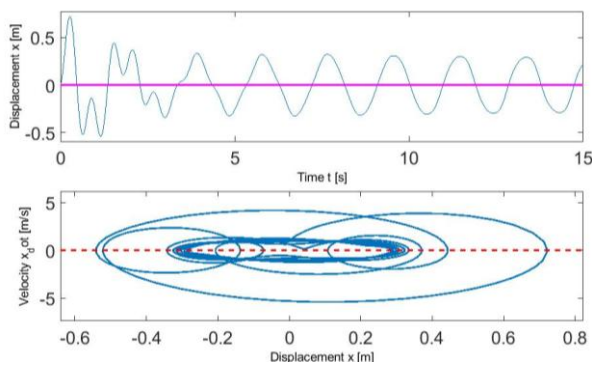


Figure 2: Displacement of mass 1 and phase diagram for the system with Coulomb friction model

The diagram presented in Figure 2 shows the displacement of mass 1 as a function of time and the velocity of mass 1 as a function of displacement x for the system with the Coulomb friction model.

The first diagram in Figure 2 shows two different parts of motion: transient motion and the steady state motion. Transient motion lasts for approximately 4 seconds. During the transient motion, the amplitude decreases.

As can be seen in Figure 2, during the transient motion, mass 1 has a positive displacement for $t \in (0, 0.428s)$, negative displacement for $t \in (0.428s, 1.359s)$, positive displacement for $t \in (1.359s, 2.272s)$ and then again negative displacement for $t \in (2.272s, 3.377s)$. Maximum displacement occurs at the beginning of motion at $t = 0.249$ s and it amounts to 0.713 m.

After transient motion decays, mass 1 settles into the steady state motion. The frequency of the steady state motion

is equal to the forcing frequency (frequency of the weightless plate).

The second diagram in Figure 2 represents space-phase diagram, where the velocity of mass 1 is plotted on y-axis as a function of the displacement x . Mass 1 has a velocity at the beginning of motion according to the initial conditions.

The diagram presented in Figure 3 shows the displacement of mass 2 as a function of time and the velocity of mass 2 as a function of displacement y for the system with the Coulomb friction model.

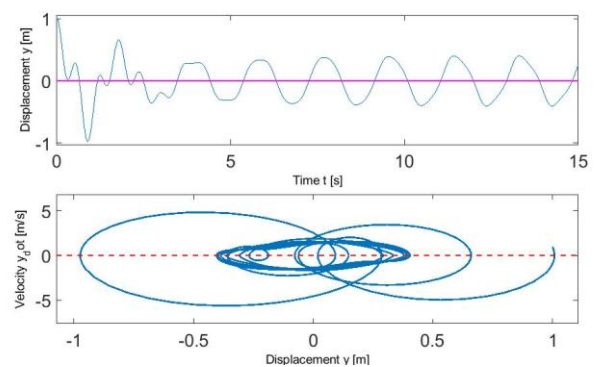


Figure 3: Displacement of mass 2 and phase diagram for the system with Coulomb friction model

The first diagram in Figure 3, same as before, shows two different parts of motion: transient motion and steady state motion. Transient motion lasts for approximately 3 seconds. During the transient motion, the amplitude decreases.

At the beginning of motion, mass 2 exhibits displacement of 1m according to the initial conditions. During the transient motion, mass 2 has positive displacement for $t \in (0, 0.646s)$, negative displacement for $t \in (0.646s, 1.182s)$, positive displacement for $t \in (1.182s, 1.342s)$, negative displacement for $t \in (1.342s, 1.541s)$, positive displacement for $t \in (1.541s, 2.083s)$, negative displacement for $t \in (2.083s, 2.185s)$, positive displacement for $t \in (2.185s, 2.522s)$ and again negative displacement for $t \in (2.522s, 3.481s)$. Maximum displacement, excluding the initial displacement, occurs at $t = 0.884s$ and it amounts to 0.97 m (in negative direction).

After transient motion decays, mass 2 settles into the steady state motion. The frequency of the steady state motion is equal to the forcing frequency.

The second diagram in Figure 3 represents space-phase diagram, where the velocity of mass 2 is plotted on y-axis as a function of the displacement y . Mass 2 has a velocity at the beginning of motion according to the initial conditions.

B) Coulomb viscous model

The diagram presented in Figure 4 shows the displacement of mass 1 as a function of time and the velocity of mass 1 as a function of displacement x for the system with the Coulomb viscous model.

The first diagram in Figure 4 shows two different parts of motion: transient motion and steady state motion. Transient motion lasts for approximately 3 seconds. During the transient motion, the amplitude decreases.

During the transient motion, mass 1 has positive displacement for $t \in (0, 0.479s)$, negative displacement for $t \in (0.479s, 1.340s)$, positive displacement for $t \in (1.340s, 2.924s)$ and then again negative displacement for $t \in (2.924s, 3.373s)$. Maximum displacement occurs at the beginning of motion at $t = 0.295s$ and it is approximately 0.703 m.

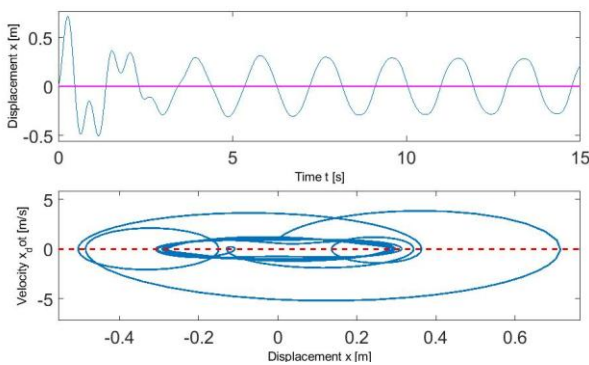


Figure 4: Displacement of mass 1 and phase diagram for the system with Coulomb viscous model

After transient motion decays, mass 1 settles into steady state motion. The frequency of the steady state motion is equal to the forcing frequency.

The second diagram in Figure 4 represents space-phase diagram, where the velocity of mass 1 is plotted on y-axis as a function of the displacement x . Mass 1 has a velocity at the beginning of motion according to the initial conditions.

The diagram presented in Figure 5 shows the displacement of mass 2 as a function of time and the velocity of mass 2 as a function of displacement y for the system with the Coulomb viscous model.

The first diagram in Figure 5 shows two different parts of motion: transient motion and steady state motion. Transient motion lasts for approximately 3 seconds. During the transient motion, the amplitude decreases.

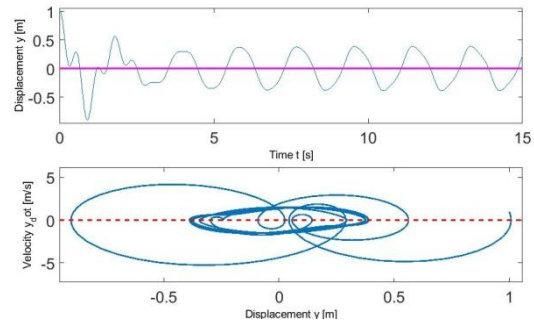


Figure 5: Displacement of mass 2 and phase diagram for the system with Coulomb viscous model

At the beginning of motion, mass 2 has a displacement of 1m according to the initial conditions. During the transient motion, mass 2 has a positive displacement for $t \in (0, 0.656s)$, negative displacement for $t \in (0.656s, 1.507s)$, positive displacement for $t \in (1.507s, 2.470s)$ and then again exhibits negative displacement for $t \in (2.470s, 3.502s)$. Maximum displacement, excluding the initial displacement, occurs at $t = 0.904s$ and it amounts to 0.904 m (in negative direction).

After transient motion decays, mass 2 settles into the steady state motion. The frequency of the steady state motion is equal to the forcing frequency.

The second diagram in Figure 5 represents space-phase diagram, where the velocity of mass 2 is plotted on y-axis as a function of displacement y . Mass 2 has a velocity at the beginning of the motion according to the initial conditions.

C) Coulomb-Stribeck model

The diagram presented in Figure 6 shows the displacement of mass 1 as a function of time and the velocity of mass 1 as a function of displacement x for the system with the Coulomb-Stribeck model.

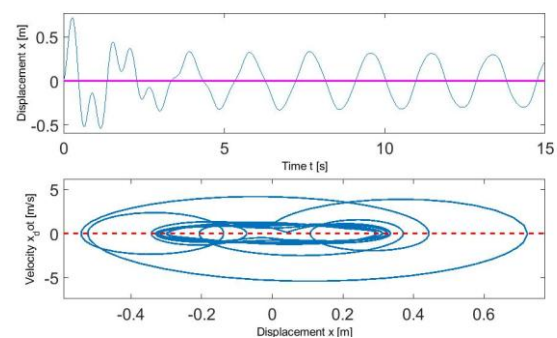


Figure 6: Displacement of mass 1 and phase diagram for the system with Coulomb-Stribeck model

The first diagram in Figure 6 shows two different parts of motion: transient motion and steady state motion. Transient

motion lasts for approximately 3 seconds. During the transient motion, the amplitude decreases.

During the transient motion, mass 1 has positive displacement for $t \in (0, 0.445s)$, negative displacement for $t \in (0.445s, 1.359s)$, positive displacement for $t \in (1.359s, 2.289s)$ and then again negative displacement for $t \in (2.289s, 3.366s)$. Maximum displacement occurs at the beginning of motion at $t=0.272s$ and it is approximately 0.723 m.

After transient motion decays, mass 1 settles into the steady state motion. The frequency of the steady state motion is equal to the forcing frequency.

The second diagram in Figure 6 represents space-phase diagram, where the velocity of mass 1 is plotted on y-axis as a function of displacement x . Mass 1 has a velocity at the beginning of motion according to the initial conditions.

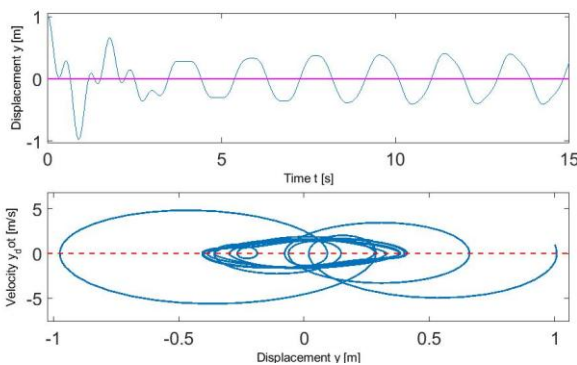


Figure 7: Displacement of mass 2 and phase diagram for the system with Coulomb-Stribeck model

The diagram presented in Figure 7 shows the displacement of mass 2 as a function of time and the velocity of mass 2 as a function of displacement y for the system with the Coulomb-Stribeck model.

The upper diagram in Figure 7 shows two different parts of motion: transient motion and steady state motion. Transient motion lasts for approximately 3 seconds. During the transient motion, the amplitude decreases.

At the beginning of motion, mass 2 has a displacement of 1m according to the initial conditions. During the transient motion, mass 2 has positive displacement for $t \in (0, 0.658s)$, negative displacement for $t \in (0.658s, 1.164s)$, positive displacement for $t \in (1.164s, 1.324s)$, negative displacement for $t \in (1.324s, 1.525s)$, positive displacement for $t \in (1.525s, 2.050s)$, negative displacement for $t \in (2.050s, 2.237s)$, positive displacement for $t \in (2.237s, 2.506s)$ and again negative displacement for $t \in (2.506s, 3.489s)$. Maximum displacement,

excluding the initial displacement, occurs at $t=0.884s$ and it amounts to 0.966 m (in negative direction).

After transient motion decays, mass 2 settles into the steady state motion. The frequency of the steady state motion is equal to the forcing frequency.

The second diagram in Figure 7 represents space-phase diagram, where the velocity of mass 2 is plotted on y-axis as a function of displacement y . Mass 2 has a velocity at the beginning of motion according to the initial conditions.

D) LuGre model

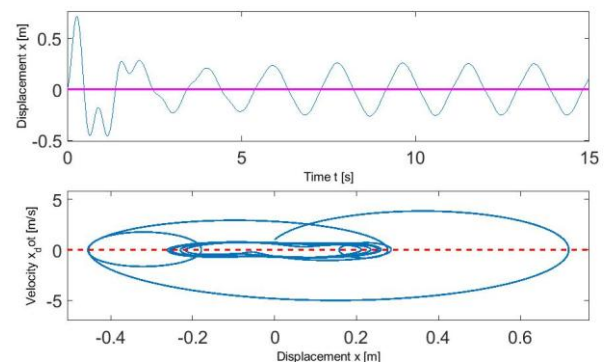


Figure 8: Displacement of mass 1 and phase diagram for the system with LuGre model

The diagram presented in Figure 8 shows the displacement of mass 1 as a function of time and the velocity of mass 1 as a function of displacement x for the system with the LuGre model.

The first diagram in Figure 8 shows two different parts of motion: transient motion and steady state motion. Transient motion lasts for approximately 3 seconds. During the transient motion, the amplitude decreases.

During the transient motion, mass 1 has positive displacement for $t \in (0, 0.475s)$, negative displacement for $t \in (0.475s, 1.356s)$, positive displacement for $t \in (1.356s, 2.439s)$ and then again negative displacement for $t \in (2.439s, 3.459s)$. Maximum displacement occurs at the beginning of motion at $t=0.292s$ and it amounts to 0.718 m.

After transient motion decays, mass 1 settles into the steady state motion. The frequency of the steady state motion is equal to the forcing frequency.

The second diagram in Figure 8 represents space-phase diagram, where the velocity of mass 1 is plotted on y-axis as a function of displacement x . Mass 1 has a velocity at the beginning of motion according to the initial conditions.

The diagram presented in Figure 9 shows the displacement of mass 2 as a function of time and the velocity of mass 2 as a function of displacement y for the system with the LuGre model.

The upper diagram in Figure 9 shows two different parts of motion: transient motion and steady state motion. Transient motion lasts for approximately 3 seconds. During the transient motion, the amplitude decreases.

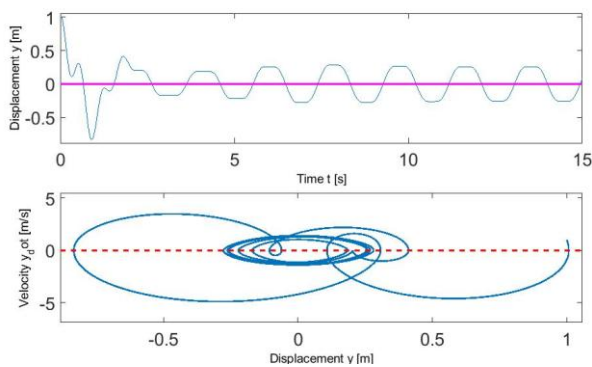


Figure 9: Displacement of mass 2 and phase diagram for the system with LuGre model

At the beginning of motion, mass 2 has displacement of 1m according to the initial conditions. During the transient motion, mass 2 has positive displacement for $t \in (0, 0.638s)$, negative displacement for $t \in (0.638s, 1.583s)$, positive displacement for $t \in (1.583s, 2.64s)$ and then again negative displacement for $t \in (2.64s, 3.66s)$. Maximum displacement, excluding the initial displacement, occurs at $t = 0.901s$ and it amounts to 0.834 m (in negative direction).

After transient motion decays, mass 2 settles into the steady state motion. The frequency of the steady state motion is equal to the forcing frequency.

The second diagram in Figure 9 represents space-phase diagram, where the velocity of mass 2 is plotted on y-axis as a function of displacement y . Mass 2 has a velocity at the beginning of motion according to the initial conditions.

IV. CONCLUSION

The vibrating responses of the two-degrees-of-freedom system with various friction models were studied in this paper. The four friction models, Coulomb, Coulomb viscous, Coulomb-Stribeck and LuGre model, were used to investigate the qualitative change of the system dynamics in different friction environments. The analysis was conducted by monitoring displacement and velocity of masses 1 and 2 during 15 seconds of motion.

The analysis has revealed minimum resistance between these friction models when the Coulomb model of friction is applied. For the Coulomb friction model, maximum displacements of masses 1 and 2 were 0.723m and 0.974m, respectively. For other three investigated models, maximum displacements were lower, meaning that the vibrations are more damped in case of other friction models than in case of Coulomb model.

Time period to reach steady state motion is similar for all friction models, with the shortest time period encountered for the Coulomb friction and the LuGre model.

The analysis gives an insight on the way different friction models may be used to decrease the oscillating amplitude and get faster to steady state motion with a constant and close to the minimum value of vibration. These properties are of high importance for dynamic absorbers. Another important characteristic is the type of motion in the steady state region. For the LuGre model, the second body in steady state motion is resting for certain time period at the maximum amplitude value. This property can be advantage for some systems while disadvantage for others. If the body needs to move quickly in the opposite direction, this feature is the disadvantage. The load on the spring will also be greater in this case, because it will be stretched and held for some time leading to a shorter lifetime.

REFERENCES

- [1] V.L. Popov, "Contact Mechanics and Friction", Springer, 2010.
- [2] B. Armstrong-Hélouvry, P. Dupont, C.C. de Wit, "A survey of models, analysis tools and compensation methods for the control machines with friction", *Automatica*, 1994.
- [3] R. Stribeck, "Die wesentlichen Eigenschaften der Gleitund Rollenlager", *Zeitschrift des Vereines Deutscher Ingenieure*, 1902.
- [4] Y. Liu, M. Wiercigroch, E. Pavlovskaja, H. Yu, "Modelling of a vibro-impact capsule system", *International Journal of Mechanical Sciences*, 66:2-11, 2013.
- [5] Y. Liu, E. Pavlovskaja, M. Wiercigroch, "Experimental verification of the vibro-impact capsule model", *Nonlinear Dynamics*, 83:1029-1041, 2016.
- [6] Y. Liu, E. Pavlovskaja, D. Hendry, M. Wiercigroch, "Vibro-impact responses of capsule system with various friction models", *International Journal of Mechanical Sciences*, 72:39-54, 2013.
- [7] Y. Liu, E. Pavlovskaja, M. Wiercigroch, Z. Peng, "Forward and backward motion control of a vibro-impact capsule system", *International Journal of Non-Linear Mechanics*, 70:30-46, 2015.

- [8] W. Sextro, “Dynamical Contact Problems with Friction”, *Springer*, 2002.
- [9] K.L.Johnson, “Contact Mechanics”, *Cambridge University Press*, 1985.
- [10] A.H. Nayfeh, D.T. Mook, “Nonlinear Oscillations”, *John Wiley & Sons Ltd*, 1995.
- [11] B. Armstrong-Hélouvy, “Control of Machines with Friction”, *Springer-Science+Business Media*, 1991.
- [12] P.J.Dolcini, C.C. de Wit, H. Béchart, “Dry Clutch Control for Automotive Applications”, *Springer*, 2010.



Dzanko Hajradinovic is Senior Research Assistant in Department of Mechanics at Mechanical Engineering Faculty of the University of Sarajevo, Bosnia and Herzegovina. He is working on a Phd thesis in the field of vibro-impact systems with non-ideal excitation. He has published 3 papers in scientific journals, as well as participated in 2 scientific conferences.



Marin Petrovic is Associate Professor in Department of Mechanics at Mechanical Engineering Faculty of the University of Sarajevo, Bosnia and Herzegovina. He was awarded PhD at University College Dublin, Ireland. He has published 3 university books and 19 papers in scientific journals, as well as participated in 13 scientific conferences.

AUTHOR'S BIOGRAPHIES



Kanita Lemes is MSc student at Mechanical Engineering Faculty of the University of Sarajevo, Bosnia and Herzegovina.

Citation of this Article:

Kanita Lemes, Dzanko Hajradinovic, Marin Petrovic, “Numerical Analysis of a Nonlinear Vibrating Two-Degrees-of-Freedom System with Various Friction Models” Published in *International Research Journal of Innovations in Engineering and Technology - IRJIET*, Volume 4, Issue 3, pp 6-12, March 2020.
